Journal of Materials Science and Engineering B 10 (5-6) (2020) 109-123
doi: 10.17265/2161-6221/2020.5-6.003

Batch Studies for the Removal of a Hazardous Azo Dye Methyl Orange from Water through Adsorption on Regenerated Activated Carbons

Mariame Conde Asseng[1], Hermann Tamaguelon Dzoujo[1], Daniel David Joh Dina[1], Marie Annie Etoh[1], Armand Ngoungue Tchakounte[1] and Julius Ndi Nsami[2]

1. Department of Chemistry, Faculty of Science, University of Douala, Douala, P.O. BOX 24157, Douala, Cameroon

2. Department of Inorganic chemistry, Faculty of Science, University of Yaounde I, Yaoundé, P.O. BOX 812, Yaoundé, Cameroon

Abstract: The study of the performances of regenerated activated carbons for the adsorption of MO (methyl orange) in an aqueous medium was carried out with the aim to evaluate the adsorption capacities of these activated carbons. Three regenerated activated carbons issued from the unit of oil treatment of the thermal power station of Dibamba (Cameroon)-DPDC (Dibamba Power Development Company) were obtained thermally and chemically. These three samples (namely CAR 400 °C (chemical regenerated activated carbon at 400 °C), CAR 700 °C (physical regenerated activated carbon at 700 °C) and CAR 900 °C (physical regenerated activated carbon at 900 °C)) and the non-used one CA were characterized by iodine number, XRD (X-ray Diffraction) and FTIR (Fourier-transform infrared spectroscopy). MO adsorption tests were performed in batch mode; this technique allowed the study of the influence of the parameters such as: the contact time, the initial's MO concentration and the pH. Moreover, different kinetic models (first-order, pseudo-second-order and Webber and Morris intra-particle diffusion) and adsorption isotherms (Langmuir and Freundlich) are used for the evaluation of adsorption capacities. The physicochemical characterization of these adsorbents showed that they were micro-porous (iodine value: 600 mg/g) and strongly crystallized according to their regeneration pathways. The influence of the parameters revealed that the adsorption of MO is the most favorable for concentrations from 5 to 25 mg/L (for materials CA and CAR 400 °C) and 10 to 25 g/L (for materials CAR 700 °C and 900 °C); and that it was maximum in acid medium (at pH = 3 on the materials CA, CAR 400 °C, CAR 900 °C and at pH = 5 on the material CAR 900 °C). The modeling of the adsorption kinetics of MO has revealed the conformity of the kinetic model of pseudosecond-order and intra-particle diffusion for some of these materials. The study of isotherms has shown that the Langmuir isotherm best describes the adsorption of MO on most of these adsorbents.

Key words: Adsorption, regenerated activated carbon, MO, batch mode.

1. Introduction

Since the beginning of the industrial age, aquatic and terrestrial ecosystems have been under increasing anthropogenic pressure every year by the dumping of thousands of substances of various kinds within them [1].

Among these substances the presence of dyes, widely used in printing, food products, cosmetics and the textile industry is observed. In fact, the textile sector is one of six branches of activity generating half of the industrial pollution flows and effluents from this sector can be very colorful and difficult to treat once released into the environment.

This is the case of azo dyes, specifically the MO (methyl orange) commonly called helianthine which is part of this family of dyes.

Studies have shown that azo dyes are toxic, bio-accumulative, mutagenic, persistent and carcinogenic to fauna and flora and the cancer risk estimate imposes a limit concentration of 3.1 μg/L of azo dye in drinking water [2-4].

In view of this and in order to preserve our health and our environment, several physico-chemical

Corresponding author: Daniel David Joh Dina, Ph.D., physical chemistry, research field: surface chemistry.

treatments have been carried out such as: precipitation, coagulation-flocculation, electrochemical treatments, ultrafiltration, reverse osmosis, processes advanced oxidation and activated carbon adsorption [5]. The later is the most effective in the elimination of dyes but has high costs [6]. From an economic and ecological point of view, the use of regenerated activated carbon can be an alternative to overcome this limit. The objective of this work will be to evaluate the performance of regenerated activated carbon to eliminate MO in an aqueous medium and in the same way, will make this work a special feature compared to several works related to the treatment of liquid waste from textile dyers containing the sulphonated azo dyes already produced here by Kumar et al. [7] and Daoud and Benturki [8].

2. Methods

2.1 Collection of Sample and Regeneration of Industrial Activated Carbons

The granular activated carbon used in this study was collected in the oily water treatment unit of the thermal power unit of Dibamba (Littoral-Cameroun). This charcoal is made by Jacobi Company and is prepared from coconut husks. The activating agent used is phosphoric acid (H_3PO_4) and the activation is made with steam at a temperature between 800 and 1,000 °C. This granular activated carbon has the particularity that once saturated by adsorbates it can be regenerated and reused.

The used granular activated carbon was taken from a PET (polyethylene terephthalate) bottle (1.5 L), subsequently mixed with 5 L of demineralized water and allowed to stand for 24 h. It was dried at 110 °C for 24 h in an oven (MEMMERT B2162385). Using a scale, 35 g of 3 samples of pretreated coals were weighed. The first two samples were introduced into porcelain crucibles and were respectively charred at 700 and 900 °C in a brand oven (NABERTHERM 30-3,000 °C), at a rate of 10 °C/min and once the required temperature is reached, it is maintained for 30 min. After carbonization, the samples were cooled, washed with HCl (hydrochloric acid) (0.05 N), then abundantly with hot deionized water, cooled again and finally dried at 110 °C for 24 h in the oven. The procedure was the same for the third sample but with the difference that this sample was first impregnated in hexane (in a proportion of 1/2 by mass or by volume) and the whole was stirred from time to time for 24 h. After filtration, carbonization was carried out at 400 °C.

2.2 Characterization Techniques of Regenerated Activated Carbons

The various activated carbons resulting from the regeneration as well as the non-used one have undergone the characterizations: the iodine number according to the procedure of the Duchet study center which is an adaptation of the CEFIC 1989 method and the standard AWWA B 600-78 [9] for evaluating micro-porosity; XRD (X-ray diffraction) to identify the different predominant crystalline phases using a Bruker X-ray diffractomer brand diffractometer (D8 Discovery, US) at CSIR-National Metallurgical Laboratory, Jamshedpur, India, and Infra Red Fourier Transform to be able to also identify the functional groups on the surface of these materials using a Fourier transform infrared spectrophotometer (IR Nicolet IS5 de Thermo Scientific).

2.3 Chemicals and Reagents

MO dye with the molecular formula ($C_{14}H_{14}N_3O_3S^-Na^+$) and molecular weight of 327.34 g/mol is chosen as adsorbate. Its molecular structure is described by the following chemical formula:

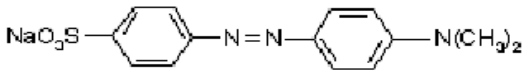

HCl and NaOH (sodium hydroxide) (Sygma Aldrich) were also used in this research work.

2.4 Adsorption Experiments

The adsorption experiments are performed in

batches at different initial values of dye concentrations and contact times. They are carried out by introducing a precisely weighed quantity of adsorbent (0.2 and 0.4 g) into a volume of 100 mL of solutions of dyes prepared previously. The solutions are then separated from the adsorbent by Whatman filter papers after stirring on a magnetic stirrer for 2 h. Subsequently the absorbance of these solutions is measured using a spectrophotometer (SCHOTT UV/visible instruments) at the wavelength corresponding to the maximum absorbance of the sample (λ = 465 nm).

The adsorption capacity and the removal rate of MO R (%) are calculated using the following formulas:

$$Q_t = ((C_0\text{-}C_t)\cdot V)/m_{CA} \quad (1)$$

$$R = ((C_0\text{-}C_t)\cdot 100)/C_0 \quad (2)$$

where, Q_t: The amount adsorbed at time t (mg/g); C_0: The initial dye concentration (mg/L); C_t: The dye concentration at time t (mg/L); V: The volume of the solution (mL) and m_{CA}: The mass of the adsorbent in solution (g).

2.5 Contact Time Experiments Studies

One hundred (100) mL of solutions of 10 mg/L is prepared. A mass of 0.4 g of each carbon is added every time in different solutions and then stirred by a magnetic stirrer during the time intervals of 5, 15, 30, 45, 60 and 75 min. Samples were taken after adsorption and filtered and the filtrates' concentrations are determined by UV/visible spectrophotometer.

2.6 Influence of MO Concentration Experiments Studies

Twenty (20) mg of different coals samples are added alternately to 100 mL in each of the six MO solutions whose initial concentrations are 5, 10, 15, 20, 25 and 30 mg/L and stirred on the shaker with magnetic stirrer at different fixed times. The mixtures are then filtered and the filtrates' concentrations are determined by the UV/visible spectrophotometer.

2.7 pH Experiments Studies

pH is an important factor in any adsorption study because it can influence both the adsorbent and adsorbate structure as well as the adsorption mechanism.

In this work the pH was measured using a pH-meter HANNA instrument, the adsorption efficiency of MO by varying the pH from 0 to 10 using a solution of HCl (0.1 N) or NaOH (0.1 N) depending on the desired pH was studied. Under these pH conditions, 0.2 g of the adsorbent was stirred in 100 mL of the 10 mg/L concentration of dye solution for a fixed time.

3. Results and Discussion

3.1 Results of the Characterizations of the Different Samples of Activated Carbons

3.1.1 Iodine Number

Based on the procedure of the Duchet Study Center (which is an adaptation of the CEFIC 1989 method and the AWWA B 600-78 standard), the iodine numbers of the 4 different samples (the non-used one and the regenerated activated carbons) have been determined and the results are presented in Table 1, it is found that the samples have an iodine value greater than 600 mg/g. According to the specifications of AWWA B 600-78 [9], activated carbons with an iodine number greater than or equal to 600 mg/g are recommended for drinking water. And also the microporosity of CAR 400 °C coal is close to that of CA (the non-used activated carbon) proving that hexane has perfectly played its role of desorption agent. As for the coals regenerated physically at 700 °C and 900 °C, the microporosity is not great as for the two first samples, this can be explained by the fact that at high temperatures the carbon skeleton of those samples solid began to self-distruct.

Table 1 Iodine numbers of the different samples.

Samples	CA	CAR 400 °C	CAR 700 °C	CAR 900 °C
Iodine number (mg/g)	1,052	1,045	748	880

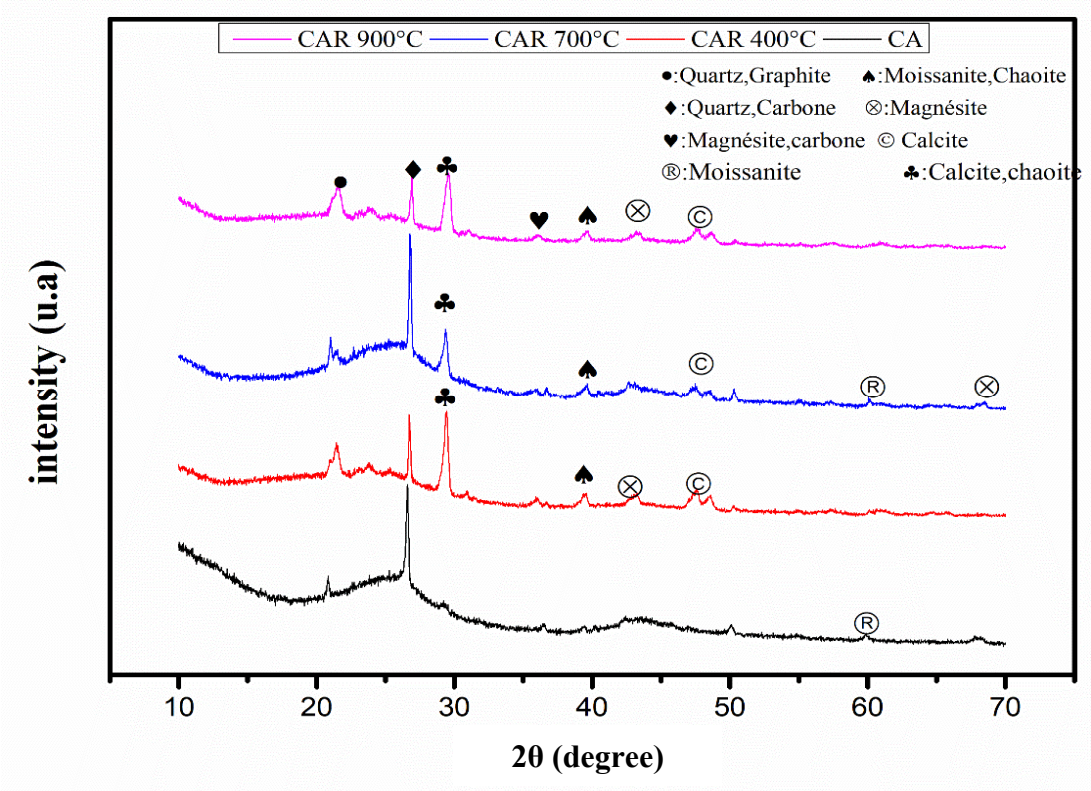

Fig. 1 XRD patterns of coals CA, CAR 400 °C, CAR 700 °C and CAR 900 °C.

Table 2 XRD analysis results.

2θ (degree)	d_{hkl} (Å)	Phases cristallines
20.98	4.23	Quartz (S_iO_2), Graphite (C)
26.84	3.31	Quartz (S_iO_2), Carbone (C)
29.38	3.03	Calcite (C_aCO_3), Chaoite (C)
36.02	2.49	Magnésite ($MgCO_3$), Carbone (C)
36.79	2.44	Moissanite (S_iC)
39.78	2.26	Moissanite (S_iC), Chaoite (C)
47.63	1.90	Calcite (C_aCO_3)
50.83	1.80	Quartz (S_iO_2), Graphite (C)
60.12	1.53	Calcite (C_aCO_3), Moissanite (S_iC)
68.64	1.36	Magnésite ($MgCO_3$)

3.1.2 XRD Analysis

The diffractograms obtained for different carbons (CA, CAR 400 °C., CAR 700 °C and CAR 900 °C) by XRD as well as the various crystalline phases are shown in Fig. 1 and Table 2. The identification of different groups of minerals from the inter-reticular distances was made on basis of ASTM (American Society for Testing and Materials) files and the original pattern of the identified minerals [10]. The analysis of the diffractograms indicates an influence of the crystalline state, these diffractograms are distributed as follows: a first concave zone between 16° and 34.6° representing the amorphous phase of the different coals. But in this amorphous phase the presence of some peaks of crystallization appearing at 20.98°, 26.84° and 29.388° corresponding respectively at inter-reticular distances respectively of 4.23 Å, 3.3184 Å and 3.0367 Å is observed. These inter-reticular distances correspond to the crystalline phases of carbons, quartz and calcites on the materials CAR 400 °C, CAR 700 °C and CAR 900 °C, but the peak at 29.388° is not observed on the non-used

activated carbon CA.

The second zone between 34.6° and 70° mainly presents peaks of crystallization on the different materials whose different crystalline phases have been observed (Table 2).

It emerges from these diffractograms that quartz is the major element of these coals and that the regeneration temperatures (400 °C, 700 °C and 900 °C) of these coals are at the origin of the absence or the appearance of crystallization peaks within them thus showing that the regeneration has modified the structural properties of the base material (CA). These results are almost similar to those found by Girgis et al. [11] in the study of XRD patterns of activated carbons prepared under various conditions.

3.1.3 Functional Groups Analysis by FTIR (Fourier-Transform Infrared Spectroscopy)

The FTIR spectra in Fig. 2, as well as the infrared bands were displayed by this infrared spectroscopy between 4,000 and 400 cm^{-1}.

The FTIR spectrum of the non-used carbon CA has peaks at 3,800 and 3,580 cm^{-1} attributable respectively to the O-H, N-H stretching bonds of the phenolics, amides of the acid sites of the coal. The peaks that are remarkably evolving in the 2,920, 2,850, 2,400 and 2,300 cm^{-1} regions are attributable respectively to the aliphatic C-H elongation band and the elongation of the nitriles. The peaks observed in the 1,750 and 1,490 cm^{-1} regions are attributable respectively to the C=O and C=C bonds of the alkenes, aromatic groups, amines, carbonyls, amides and carboxylic acids. Those between 1,300 and 1,000 cm^{-1} are attributable to aromatic C-N and C-O groups. And lastly, the peaks evolving remarkably in the 1,000-600 cm^{-1} regions correspond to the deformation bands outside the C=C plane of the alkenes and C-H of the aromatics.

The FTIR spectrum of the CAR 700 °C sample differs from that of the non-used activated carbon sample (CA) with the absence of the peak at 660 cm^{-1} due to the fact that some sites of adsorption are always occupied by adsorbates.

As for the FTIR spectrum of the CAR 900 °C sample, it is almost identical to that of the basic spectrum, thus showing that the desorption was made but differed to it with the appearance of a peak at 600 cm^{-1}. This can be explained by the fact that at this temperature (900 °C) the bonds of the functions present at the surface of the solid tend to be more deformed.

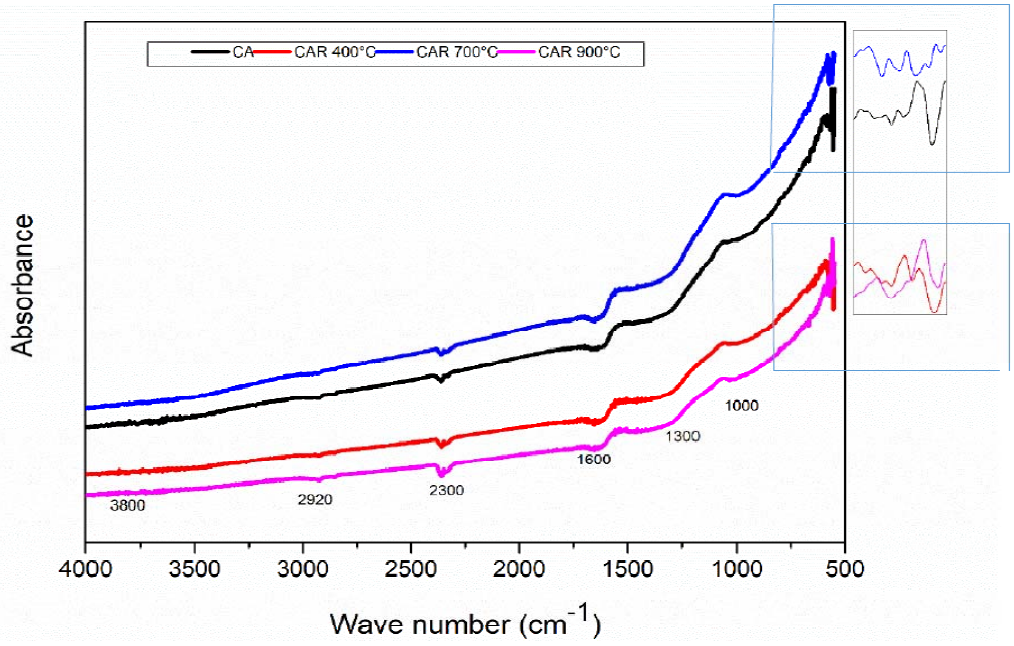

Fig. 2 FTIR spectra of non-use and regenerated activated carbons samples.

The FTIR spectrum of the CAR 400 °C sample is similar to that of the non-used material despite the appearance of the weak peak at 600 cm^{-1}. Hexane impregnation and regeneration temperature have certainly played a very important role in the restoration of active sites. This is also confirmed by the result of iodine numbers obtained on this material (Table 1).

For all the 4 samples, C=O and C-O groups are observed confirming the carbonate crystalline phases determined by the XRD and these will be responsible for the bonds between the adsorbate and the adsorbent during the adsorption process [12].

3.2 Influence of the Different Parameters

3.2.1 Influence of Contact Time

The experiments are carried out according to the procedure described above; to do this the stirring time is varied while keeping constant the concentration of the solution (10 mg/L), the mass of the different carbons at 0.4 g and ambient temperature. Figs. 3 and 4 present the results of the kinetic study as well as those of the rate of elimination of the dye on different coals.

It is noted that for the different samples of coals (AC, CAR 400 °C, CAR 700 °C, CAR 900 °C) the adsorptions capacities and the removal rates in MO increase rapidly with time and then stabilize, these stabilizations are marked respectively by equilibrium times of 60 min stirring for CA coal, 15 min for CAR 700 °C, 90 min of stirring for CAR 400 °C and 12 min of stirring for CAR 900 °C charcoal.

In view of these different analyses, the equilibrium time observed proves that the samples do not have the same textural properties which are confirmed by the results of iodine numbers obtained. However, the adsorbed amounts (Fig. 3) and the removal rates (Fig. 4) at the equilibrium of the carbons CA, CAR 400 °C, CAR 700 °C and CAR 900 °C are almost identical: 2.49 mg/g, 2.49 mg/g, 2.42 mg/g and 2.44 mg/g, respectively; for respective 99.7%, 99.6% and 96.8% and 97.5% dye removal rates, showing that the surface functional groups of these samples are not different (see FTIR and XRD results) but differ with structural properties (iodine numbers results). However, this does not affect the adsorption capacities because there is a compensation between the nature of surfaces and structures of these surfaces. Nevertheless on CAR 900 °C coal, the phenomenon of desorption is

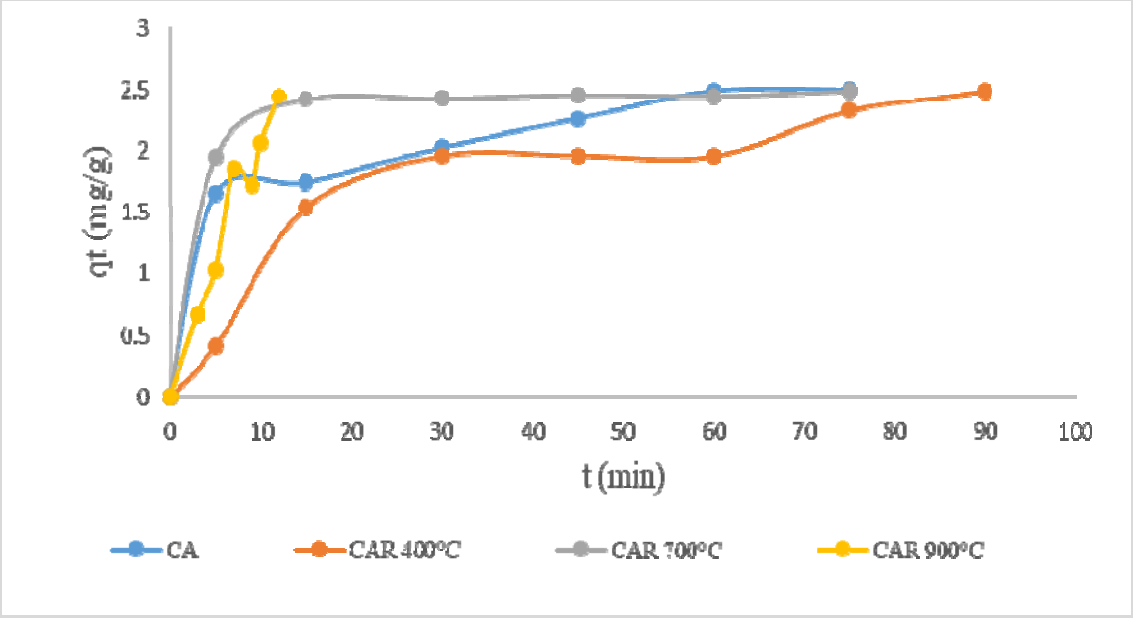

Fig. 3 Influence of the contact time on the adsorption capacity of MO on coals CA, CAR 400 °C, CAR 700 °C and CAR 900 °C. Experimental conditions: m = 0.4 g, p_i = 10 mg/L, T = 25 °C.

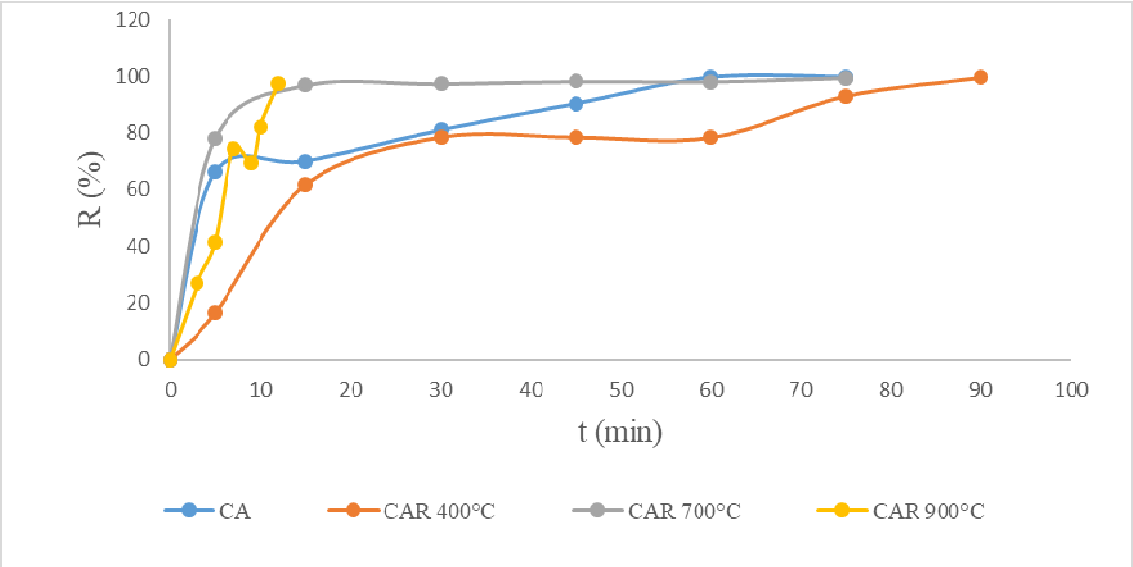

Fig. 4 The rate of removal of MO on different coals CA, CAR 400 °C, CAR 700 °C and CAR 900 °C depending on the contact time. Experimental conditions: m = 0.4 g, p_i = 10 mg/L, T = 25 °C.

very pronounced. This may be due to the fact that during physical regeneration, the high temperature (900 °C) has generated a high ash content on this material thus decreasing its adsorption capacity.

3.2.2 Influence of Initial Concentration of MO

Figs. 5a and 5b show the results of the influence of the concentration as well as those of the dye removal rate on the adsorption capacity of different coals.

From these figures it can be seen that the adsorbed amount of the MO at equilibrium increases for the concentrations greater than or equal to 25 mg/L on AC carbons, CAR 400 °C, CAR 700 °C and for concentrations less than or equal to 20 mg/L on CAR 900 °C carbon; this is due to the fact that the diffusion of dye molecules on the surface of the adsorbent was accelerated by the increase of these concentrations [13]. There is also a decrease in the amount adsorbed at equilibrium for concentrations greater than 20 mg/L and 25 mg/L respectively on CAR 900 °C and on CA, CAR 400 °C, CAR 700 °C due to the saturation of adsorptions sites on the surfaces of these materials.

On the other hand, it is found that the rate of removal in MO decreases as the concentration of increases on the carbons CA, CAR 400 °C revealing a gradual saturation of the adsorption sites on the surfaces of these adsorbents [14]. While on CAR 700 °C and CAR 900 °C, this removal rate in MO decreases for concentration ranges (5-10 mg/L, and 20-30 mg/L); and increases in the concentration range (10-20 mg/L). This decrease and increase in the removal rate in MO respectively indicate a saturation of the adsorption sites and a possible availability of a few pores or functional groups during the adsorption process in these concentration ranges.

3.2.3 Influence of pH

The results relating to the effect of pH on the adsorption of MO on different studied materials are shown in Fig. 6. It is observed that in acidic medium, that is in the pH range (0-3), the adsorption is favorable on the materials CA, CAR 400 °C, CAR 900 °C and in the pH range (0-3) and (4-5) for charcoal CAR 700 °C. These results in acid medium are almost similar to those found on the adsorption of MO on Maghnia clay by Djebbar [15]. On the other hand, a slightly favorable adsorption is observed in basic medium on the regenerated materials CAR 400 °C and CAR 900 °C in the pH range (8-10). However, the adsorption is stable on the carbons CA, CAR 400 °C and CAR 700 °C in the pH range (5-8) reflecting an adsorption equilibrium of the MO between the positive charge sites and the negative charge sites of its adsorbents. A low adsorption is

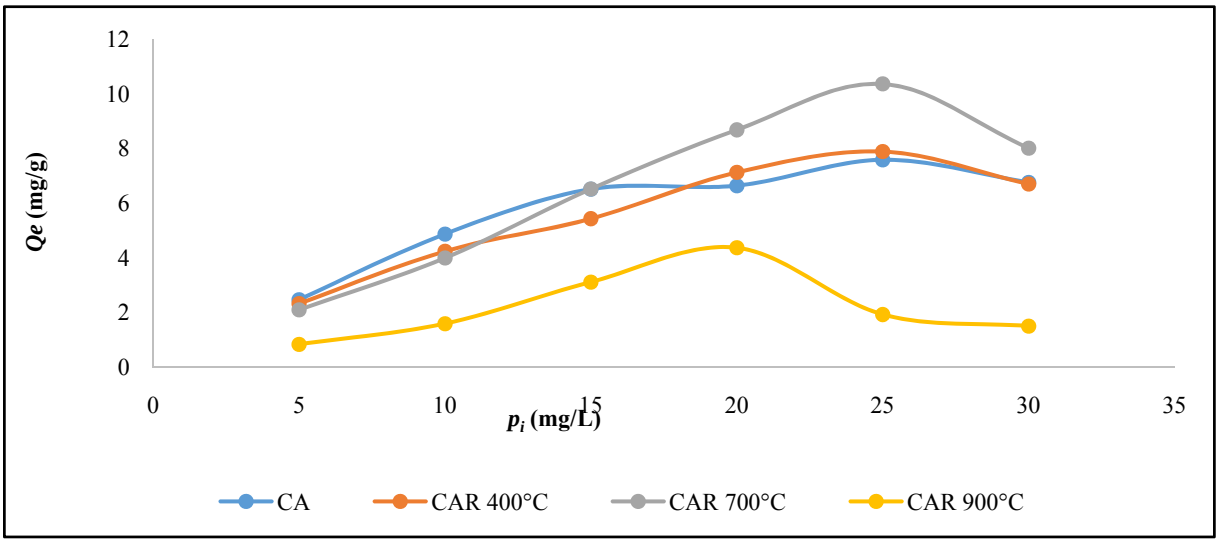

(a)

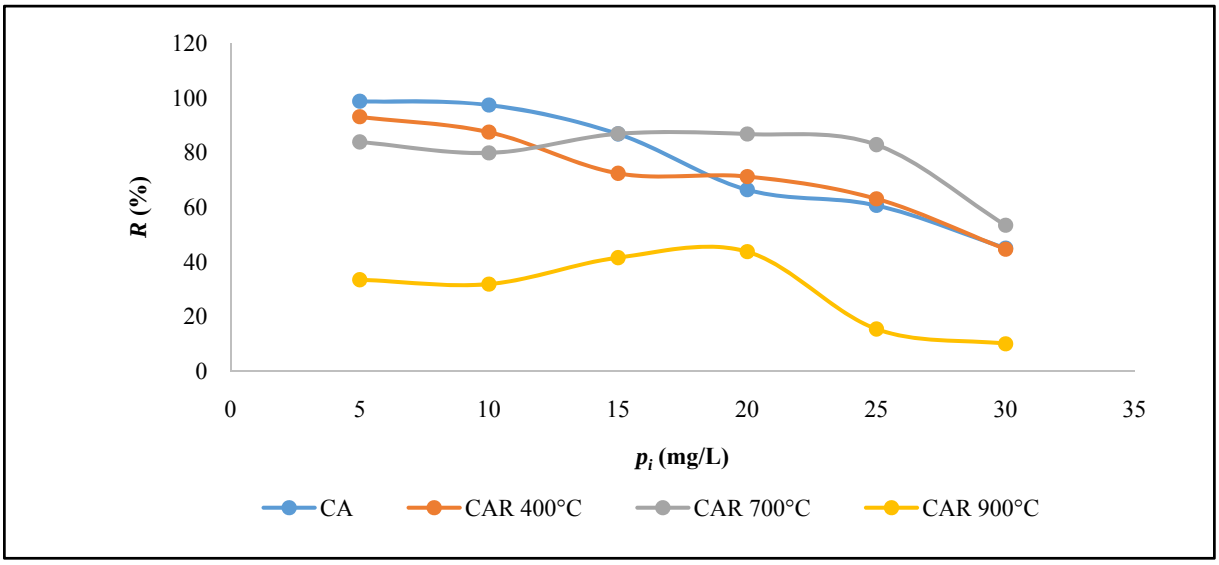

(b)

Fig. 5 (a) Influence of the initial concentration of MO on the adsorption capacity on the various coals (CA, CAR 400 °C, CAR 700 °C and CAR 900 °C); (b) The rate of removal of MO on different coals (CA, CAR 400 °C, CAR 700 °C and CAR 900 °C) depending on the concentration. Experimental conditions: m = 0.2 g, T = 25 °C, t = 75 min for CA, CAR 400 °C, CAR 700 °C and t = 15 min for CAR 900 °C.

observed in the pH ranges (3-5, 4-5 and 8-10) on the carbons CA, CAR 400 °C, CAR 700 °C and CAR 900 °C translating an electrostatic repulsion of charges of the same sign between the adsorbent and the adsorbate.

In view of these observations, it should be noted that the strong adsorption of the MO in acidic medium is explained by the electrostatic attraction at the solid-liquid interface between the positive charge of the adsorbate supplied during the addition of the acid (HCl) and the negative loading sites of the adsorbent favored by the increase in the density of the acidic groups and the basic character of these materials [16].

3.3 Results Obtained from the Different Kinetic Models

In order to examine the adsorption mechanism, the kinetic models of pseudo first-order, pseudo second-order

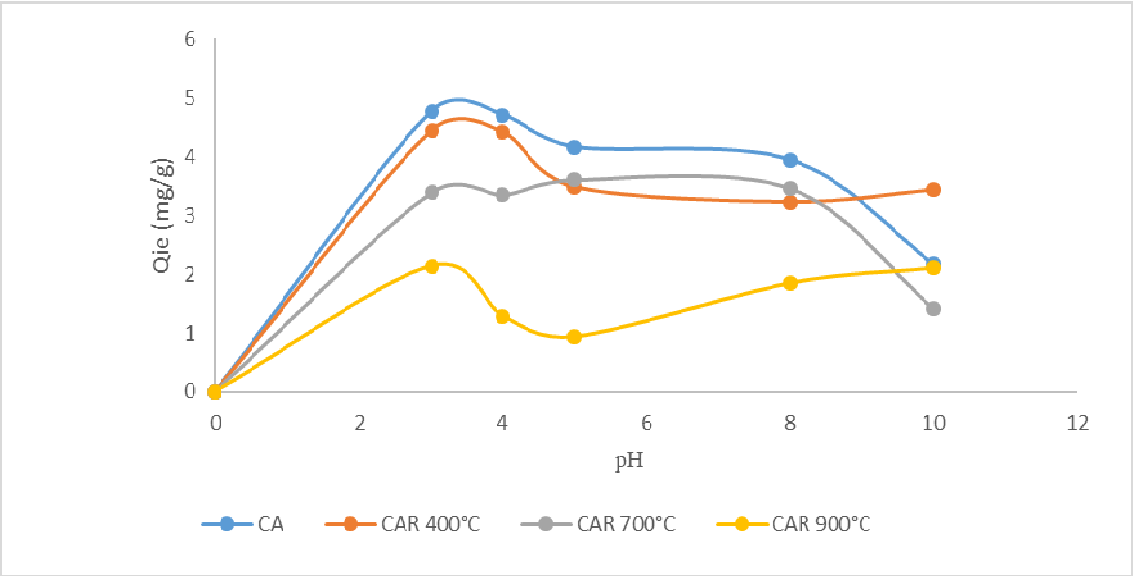

Fig. 6 Influence of pH on the adsorption capacity of the MO on different carbons according to the pH. Experimental conditions: m = 0.2 g, p_i = 10 mg/L, T = 25 °C.

and intra-particle diffusion were used to test dynamic experimental data.

3.3.1 Pseudo-First-Order Model or Lagergren Model

It has been assumed that in this model, the sorption rate at time t is proportional to the difference between the equilibrium adsorbed quantity q_{eq} and the quantity adsorbed at that time and that the adsorption is reversible [17]. The rate law is written as follows:

$$dq_t/dt = K_1(q_e-q_t) \quad (3)$$

where q_e and q_t are respectively the quantities of the dye (mg/g) adsorbed at equilibrium and at time t. K_1 is the rate constant (min^{-1}). By integrating and applying the initial conditions (at $t = 0$, $q_t = 0$ and $t = t_e$, $q_t = q_e$), the previous equation takes the form:

$$\log(q_e-q_t) = -(K_1/2.303)t + \log q_e \quad (4)$$

K_1 and q_e are obtained by representing $\log(q_e-q_t)$ as a function of t.

3.3.2 Pseudo-Second-Order Model

Ho and McKay [18] presented a model to characterize the kinetics of adsorption taking into account both the case of a rapid fixation of solutes at the most reactive sites and that of a slow fixation at the weak sites energies. The rate law is written as follows:

$$dq_t/dt = K_2(q_e-q_t)^2 \quad (5)$$

K_2 is the pseudo-second-order rate constant (g/(mg·min)).

By integrating and applying the conditions (at $t = 0$, $q_t = 0$ and $t = t_e$, $q_t = q_e$), the preceding equation takes the linear form follows:

$$t/q_t = (1/q_e)t + (1/K_2q_e^2) \quad (6)$$

q_e and k_2 are obtained by representing t/q_t as a function of t.

3.3.3 Intra-Particle Diffusion Model

This model was proposed by Weber and Morris. The molecule is supposed to migrate by diffusion into the liquid and penetrate into the pores along the axis of these pores. Along the way it equilibrates locally along the wall by adsorption, it is represented by Eq. (7):

$$q_t = K_{id}t^{1/2} + C \quad (7)$$

where: K_{id} is the intra-particle diffusion constant in mg/(g·$min^{1/2}$).

q_t: is the quantity of solutes adsorbed at time t (mg/g).

C: is the constant representative of the thickness of the diffusion boundary layer, the higher C is, the greater the effect because the boundary layer is important.

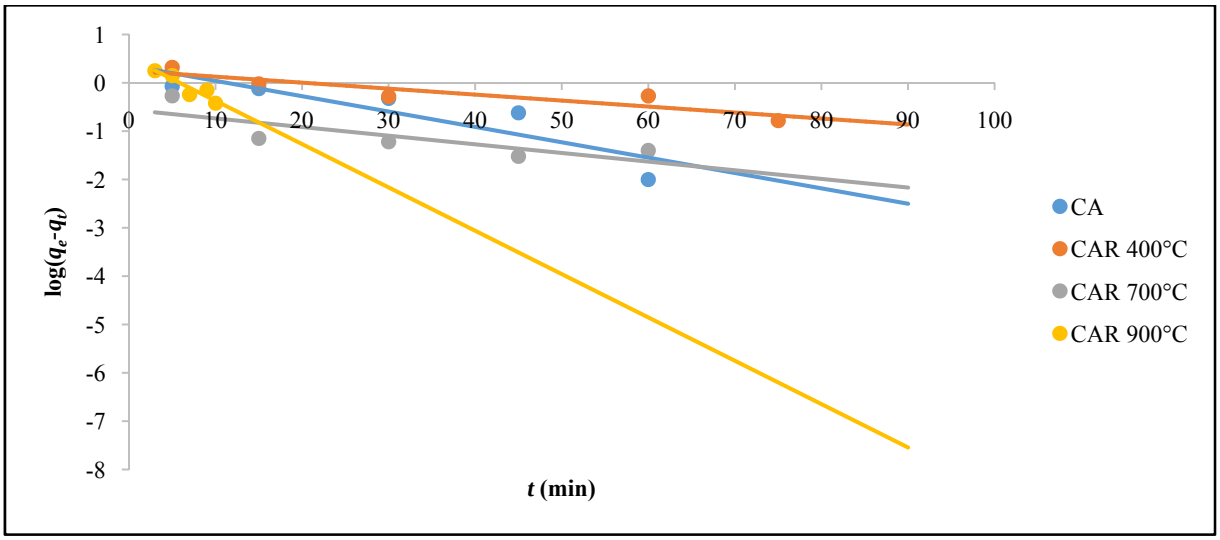

Fig. 7 Pseudo first-order kinetic model transforms plots of the adsorption of OM on materials CA, CAR 400 °C, CAR 700 °C and CAR 900 °C. Experimental conditions: m = 0.4 g, p_i = 10 mg/L, T = 25 °C.

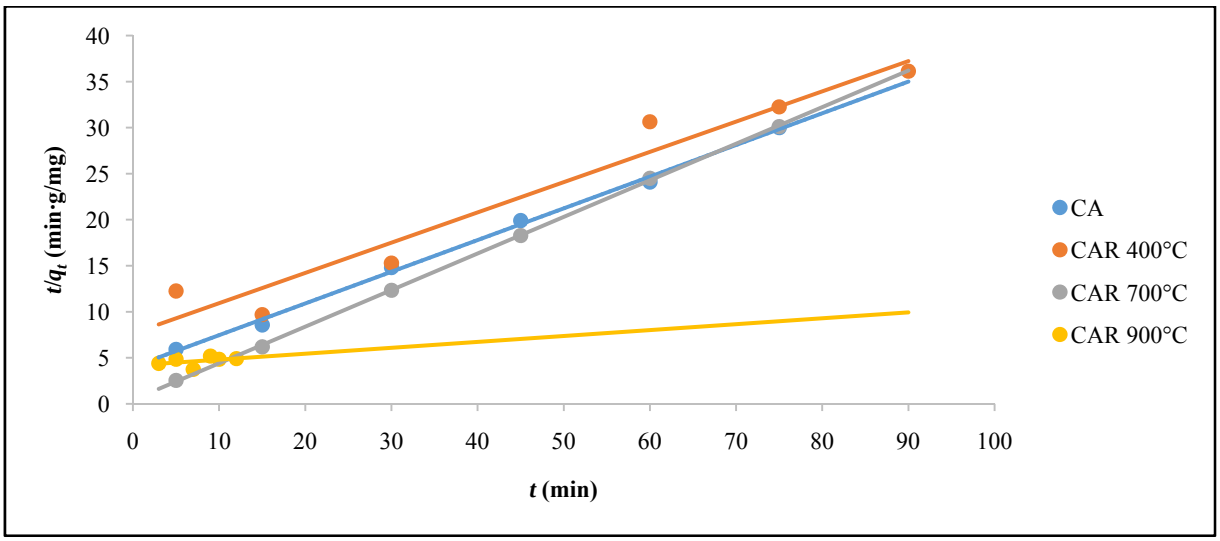

Fig. 8 Pseudo second-order kinetic model transform plots of the adsorption of MO on materials CA, CAR 400 °C, CAR 700 °C and CAR 900 °C. Experimental conditions: m = 0.4 g, p_i = 10 mg/L, T = 25 °C.

Figs. 7-9 and Table 3 present the different plots and parameters of pseudofirst-order, pseudo second-order and intraparticle diffusion kinetics models used to examine the mechanisms of control of the adsorption process and predict the most appropriate kinetic model for the adsorption of MO on different coals. The kinetic model of pseudo-second order is suitable for describing the adsorption mechanism of MO on the materials CA, CAR 400 °C and CAR 700 °C because the correlation coefficients (R^2) are very close to 1 (Table 3) and this mechanism would proceed as follows: diffusion of the solute molecule towards the boundary layer, followed by the movement of these towards the interior of the pores and finally fixation of the solute on the active sites inside the particle adsorbent [19]. And with this model it can be suggested that it is chemical adsorption type that is real chemical bond (see FTIR results in Fig. 2) between functional groups observed on the surfaces of the coals and the MO. As for the CAR 900 °C material, the intra-particle diffusion model is suitable for describing MO adsorption mechanism at its

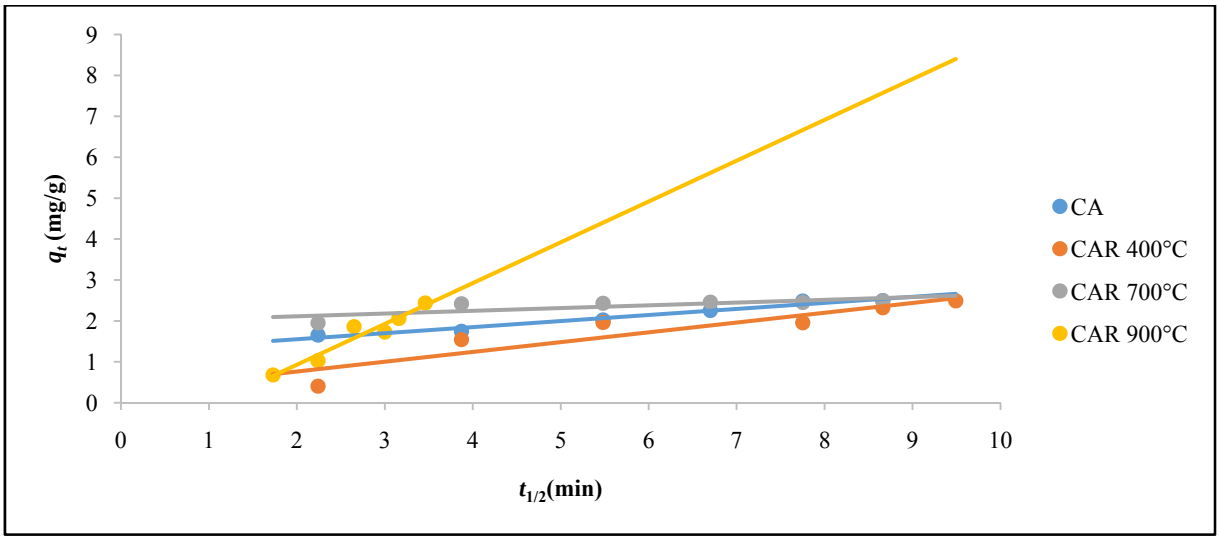

Fig. 9 Intra-particular diffusion model transform plots of the adsorption of MO on materials CA, CAR 400 °C, CAR 700 °C and CAR 900 °C. Experimental conditions: m = 0.4 g, p_i = 10 mg/L, T = 25 °C.

Table 3 Values of the correlation coefficients of the different kinetic models in linearity with the experimental results and calculated values of some kinetics parameters.

Models	Lagergren		Pseudo-second order		Intra-particle scattering		
Activated carbons	K_1 (min^{-1})	R^2	K_2 (g/(mg·min)	R^2	K_{id} (mg/(g·$min^{1/2}$))	C	R^2
CA	0.07	0.78	0.03	0.99	0.1479	1.2579	0.96
CAR 400 °C	0.02	0.83	0.01	0.95	0.2397	0.2834	0.84
CAR 700 °C	0.04	0.65	0.37	0.99	0.0669	1.9798	0.62
CAR 900 °C	0.21	0.86	98×10^{-6}	0.14	0.9977	-1.0671	0.93

surface because the correlation coefficient (R^2) is very close to 1 unlike other kinetic models and this mechanism suggests that the molecules migrate by diffusion into the liquid and penetrate into the pores along the axis thereof. Similar results have been obtained by several researchers as Hameed [20] and Hameed et al. [21, 22].

3.4 Adsorption Isotherms

The adsorption isotherm is the characteristic curve of the change in the amount Q_e adsorbed on equilibrium solid as a function of the equilibrium concentration C_e of the adsorbable compound (Q_e = f(C_e), at a given temperature. Thus, the shape of the curve obtained makes it possible to make hypotheses the mechanisms involved: adsorption in monolayer or in multilayer, interaction between adsorbed or non-adsorbed molecules.

3.4.1 Langmuir Model

The Langmuir isotherm is based on the simplest adsorption model representing the formation of a single layer. It satisfactorily represents the type I isotherms. This model was initially developed to represent the chemisorption phenomena on localized adsorption sites. This model is based on several hypotheses [23]:

- The adsorption sites on the surface of the solid are all energetically equivalent;
- Each site can only fix one molecule;
- The adsorption is done in monolayer;
- There is no interaction between the adsorbed molecules.

Under these conditions, the isotherms can be modeled by the equation as follows:

$$Q_e = \frac{Q_{max} K_L C_e}{1 + K_L C_e} \quad (8)$$

where Q_e: amount adsorbed at equilibrium (mg/g); Q_{max}: maximum adsorbable quantity (mg/g); K_L: Langmuir constant (L/mg); C_e: concentration in the liquid phase at equilibrium (mg/L). Q_{max} is the maximum amount of adsorbate that can be fixed indicating a total occupation of the adsorption sites. On the other hand, the Langmuir K_L constant, which depends on the temperature, gives an indication of the affinity of the adsorbate for the adsorbent: the higher it is, the stronger the affinity. The linearization of the Langmuir equation is:

$$\frac{C_e}{Q_e} = \frac{1}{K_L Q_{max}} + \frac{1}{Q_{max}} C_e \quad (9)$$

Q_{max} and K_L are determined by representing C_e/Q_e as a function of C_e.

The Lanmuir parameter K_L permits to express the adimensional parameter R_L called separator factor as follows:

$$R_L = \frac{1}{(1 + K_L C_0)} \quad (10)$$

where C_0: the initial concentration of the adsorbate.

If $R_L = 0$, the adsorption is irreversible; if $0 < R_L < 1$, then the adsorption is favorable; if $R_L = 1$, it is linear and if $R_L > 1$, it is unfavorable.

3.4.2 Freundlich Model

This established relationship for gas adsorption has been, and still is, widely used to describe the adsorption of solutes on solids. It is intended to describe the adsorption on heterogeneous surfaces (whose adsorption sites are not all equivalent) considering that it results from the adsorption on a large number of homogeneous small surfaces described [24]. It is written as follows:

$$Q_e = K_F C_e^{1/n}, \text{ with } n > 1 \quad (11)$$

where, Q_e: amount adsorbed at equilibrium (mg/g); C_e: equilibrium concentration (mg/L), K_F: Freundlich's constant (L/g) and n: Freundlich's coefficient.

K_F and n are two coefficients whose meaning is not immediately accessible, indicating simply that K_F depends on the total number of adsorption sites and that n is a function of the distribution of adsorption energies; when their values are very high, they reflect a strong adsorption of solutes. The linearization of this model is defined by:

$$\ln(Qe) = \ln K_F + \frac{1}{n} \ln C_e \quad (12)$$

n and K_F are obtained by the plot $\ln Q_e = f(\ln C_e)$.

In order to search for the different mechanisms involved, the experimental results obtained previously were compared with the theoretical models of Langmuir and Freundlich. Figs. 10 and 11 and parameters (Table 4) were obtained from these different isotherm models. It should be noted that the assessment of the validity of the results in Table 4 is based on the value of the correlation coefficient R^2 and the different parameters of these different models. And it follows that the Freundlich model is unsuitable for describing the adsorption of MO on the carbons CA, CAR 700 °C, CAR 900 °C because the correlation coefficients obtained are very weak although the coefficients of Freundlich ($1/n$) are between 0 and 1. On the other hand, the adsorption of MO could be described with this model on the carbon CAR 400 °C because one has a good correlation of 0.91 and more the coefficient of Freundlich ($1/n$) is between 0 and 1 indicating that the adsorption is favorable on this material.

As for the Langmuir model, it seems to be the most appropriate to describe the adsorption of the dye on the carbons CA, CAR 400 °C and CAR 700 °C because they have high correlation coefficients (0.99, 0.98, 0.93 respectively) and additionally the separator factors (R_L) are between 0 and 1 indicating that the adsorption is favorable. This result also indicates that it is a monolayer adsorption and the activated sites on the surfaces of these sorbents are homogeneous. On the other hand, this model is inappropriate to describe the adsorption of this dye on the sample CAR 900 °C because weak correlation coefficient and separator factor less than 0 indicates that the adsorption is

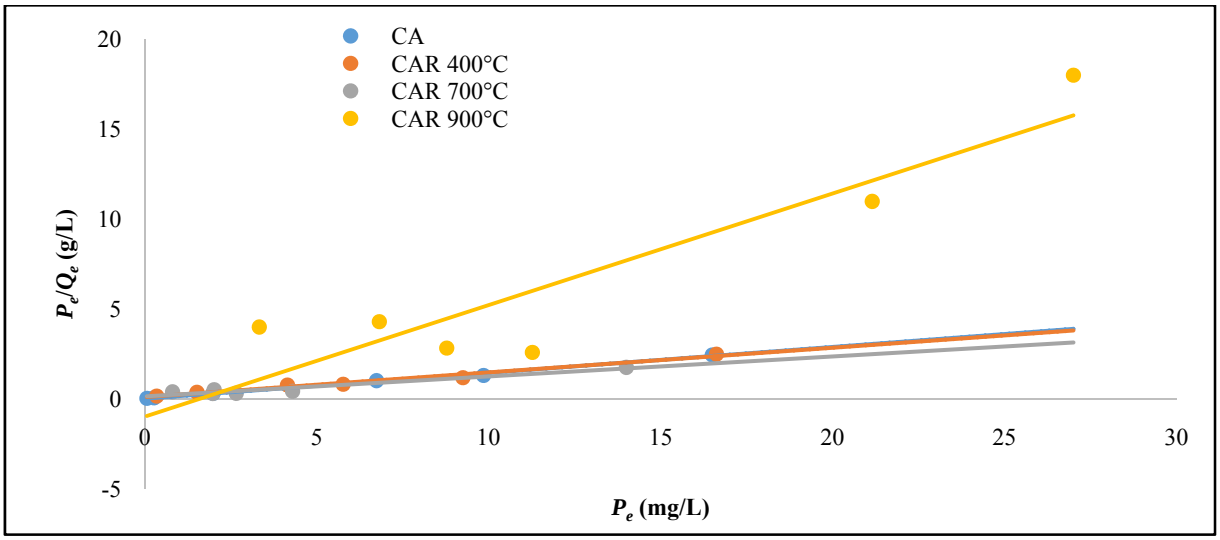

Fig. 10 Langmuir isotherm plot of the adsorption of MO on materials CA, CAR 400 °C, CAR 700 °C and CAR 900 °C. Experimental conditions: m = 0.2 g, T = 25 °C, t = 75 min for CA, CAR 400 °C, CAR 700 °C and t = 15 min for CAR 900 °C.

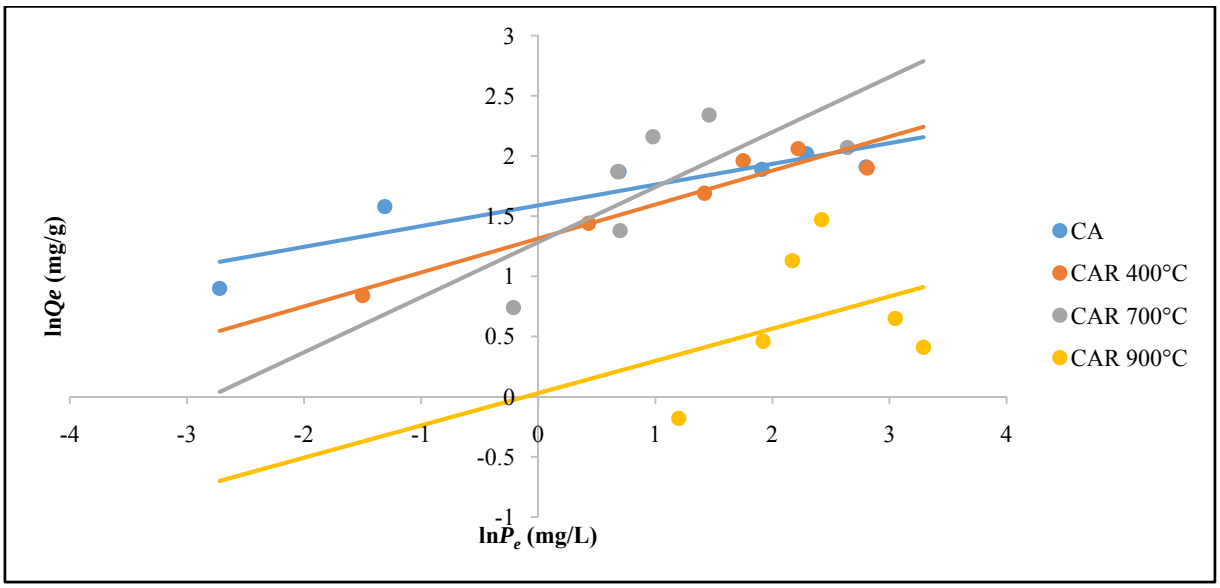

Fig. 11 Freundlich isotherm plot of the adsorption MO on materials CA, CAR 400 °C, CAR 700 °C and CAR 900 °C. Experimental conditions: m = 0.2 g, T = 25 °C, t =75 min for CA, CAR 400 °C, CAR 700 °C and t = 15 min for CAR 900 °C.

Table 4 Correlation coefficients and adsorption parameters deduced from Langmuir and Freundlich adsorption models after adsorption of MO on different coal.

Parameters	Isothermal of Langmuir				Isothermal of Freundlich		
	Q_{max} (mg/g)	K_L (L/g)	R_L	R^2	K_F (L/g)	1/n	R^2
CA	6.95	20.27	1.97×10^{-3}	0.99	4.90	0.17	0.83
CAR 400 °C	7.28	1.44	0.02	0.98	3.72	0.28	0.91
CAR 700 °C	9	0.09	0.3	0.93	3.60	0.45	0.53
CAR 900 °C	1.61	-0.39	-0.11	0.84	1.03	0.26	0.12

unfavorable. Moreover, it is found that the Langmuir constant which reflects the affinity between the material and the adsorbate decreases more and more on the different regenerated materials; this is due to the difference in regeneration temperature. Therefore, the higher the regeneration temperature, the lower the adsorption capacity.

On the other hand, none of these two isotherms describe the adsorption of MO on the CAR 900 °C coal, which suggests that the regeneration temperature (900 °C) on this material had a great impact on its carbon skeleton adversely affecting its adsorption capacity.

4. Conclusion

Determination of physicho-chemical properties of regenerated (chemically and physically) activated carbons has been done. It appears that these adsorbents are microporous, highly crystallized and have functional groups on their surfaces that will play a very important role during adsorption. The adorption of MO an azo dye commonly used in textile sector has been done. The study parameters such as: the contact time, the pH, the initial concentration of the adsorption on the various materials CA, CAR 400 °C, CAR 700 °C and CAR 900 °C permit to obtain the conditions for which adsorption is most favorable. For the different samples of coals the adsorption capacities and the removal rates in MO increase rapidly with time and then attained equilibrium at different time for each sample: 60 min for the non-used activated carbons (CA), 15 min and 12 min for the two physical regenerated activated carbons (CAR 700 °C and CAR 900 °C respectively) and 90 min for the chemical regenerated one (CAR 400 °C). A strong adsorption is also observed in acidic medium. The study of the kinetic models has shown that the adsorption of MO follows the pseudo-second order model on the carbons CA, CAR 400 °C and CAR 700 °C and the intraparticle diffusion model for the material CAR 900 °C. The study of the isotherms revealed that the Langmuir model best describes the adsorption of the dye on the materials CA, CAR 400 °C and CAR 700 °C unlike the material CAR 900 °C which does not obey any of the two adsorption models studied. It is clear for this work that the regeneration of used activated carbon modifies the structural properties of the carbons but has less effect on the adsorption capacities of the material regenerated at temperatures below 900 °C, temperature from which the adsorption capacity of the coal decreases due to the deterioration of the carbon skeleton and destruction of functional groups.

Sorption technology on regenerated activated carbons is shown to be a feasible alternative for removing dye as MO in industrial waste waters.

References

[1] Audy, S., Grosbois, C., Bril, H., Schafer, J., Kierczak, J., and Blanc, G. 2010. "Gost-Depositional Redistribution of Trace Metals in Reservoir Sediments of Mining Smeling-Impact Watershed (the Lot River, SW France)." *Applied Geochemistry* 25: 778-94.

[2] Brown, M. A., and Devito, S. C. 1993. "Predicting Azo Dye Toxicity." *Crit. Review of Environmental Science Technology* 23: 249-324.

[3] Tsuda T., Kato, Y., and Osawa, T. 2000. "Mechanism for the Peroxynitrite Scavenging Activity by Anthocyanins." *FEBS Letter* 484: 3.

[4] Ben Mansour, H., Boughzala, O., Dridi, D., Barillier, D., Chekir-Ghedira, L., and Mosrato, R. 2011. "Textile Dyes as a Source of Wastewater Contamination: Screening of the Toxicity and Treatment Method." *Journal of Water Science* 24 (3): 209-38.

[5] Ankoro, N. O., Kouotou, D., Belibi, B. P. D., Ndi, J. N., and Ketcha J. M. 2016. "Removal of Indigo Carmine Dye (IC) by Batch Adsorption Method onto Dried Cola Nut Shells and Its Active Carbon from Aqueous Medium." *International Journal of Engineering Sciences and Research Technology* 3: 874-87.

[6] Peternel, W. S., Winkler-Hechenleitner, A. A., and Gómez, P. E. A. 1999. "Adsorption of Cd (II) and Pb (II) onto Functionalized Formic Lignin from Sugar Cane Bagasse." *Bioressource Technology* 68: 95-100.

[7] Kumar, S. T., Bhoumik, N. C., Karmaker, S., Ahmed, M. G., Tchikawa, H., and Fukumori, Y. 2010. "Adsorption of Methyl Orange onto Chitosan from Aqueous Solution." *Journal Water Resource and Protection* 2: 898-906.

[8] Daoud, M., and Benturki, O. 2014. "Activation of Coal Based on Jujube Kernels and Applications to Environment: Adsorption of a Textile Dye." *Review of Renewable Energies* 14: 155-62.

[9] Van Vliet, B. M., Weber Jr, W. J., and Hozumi, H. 1980. "Modelling and Prediction of Specific Compound Adsorption by Activated Carbon and Synthetic Adsorbents." *Water Research* 14 (12): 1719-28.

[10] Benguella, B., and Yacouta-Nour, A. 2009. "Adsorption of Bezanyl Red and Nylomine Green from Aqueous Solutions by Natural and Acid-Activated Bentonite." *Desalination* 235: 276-92.

[11] Girgis, B. S., Temerk, Y. M., Gadelrab, M. M., and Abdullah, I. D. 2007. "X-Ray Diffraction Patterns of Activated Carbons Prepared under Various Conditions." *Carbon Science* 8 (2): 95-100.

[12] Caillère, S., and Hénin, S. 1964. "Mineralogy of Clays." *Soil Science* 98 (3): 208.

[13] Karagozoglu, B., Tasdemir, M., Demirbas, E., and Kobya, M. 2007. "The Adsorption of Basic Dye from Aqueous Solutions onto Sepiolite, Fly Ash and Apricot Shell Activated Carbon: Kinetic and Equilibrium Studies." *Journal of Hazardous Material* 147: 297-306.

[14] Zing, B., Belibi, B. P. D., Ankoro, N., Kouotou, D., Ndi, J. N., and Ketcha, J. M. 2016. "Batch Adsorption of Ammonium Ions from Synthetic Wastewater Using Local Cameroonian Clay and $ZnCl_2$ Activated Carbon." *International Journal of Engineering and Applied Sciences* 3: 75-85.

[15] Djebbar, M. 2014. "Maghnia Clay: Purification and Adsorption of Polluants." PhD thesis, University of Oran-Algeria.

[16] Huang, R., Liu, Q., Huo, J., and Yang, B. 2017. "Adsorption of Methyl Orange onto Protonated Crosslinked Chitosan." *Arabian Journal of Chemistry* 10: 24-32.

[17] Calvet, R. 2003. *Le sol: propiétés et fonctions*. France Agricole Editions. (in French)

[18] Ho, Y. S., and McKay, G. 1998. "Kinetics for Sorption of Dye from Aqueous Solution by Wood." *Process Safety and Environmental Protection* 76 (2): 183-91.

[19] Ofomaja, A. E. 2008. "Sorptive Removal of Methylene Blueu from Aqueous Solution Using Palm Kernel: Effect of Fibre Dose." *Biochemical Engineering Journal* 40: 8-18.

[20] Hameed, B. H. 2009. "Spent Tea Leaves: A New Non-conventional and Low-Cost Adsorbent for Removal of Basic Dye from Aqueous Solutions." *Journal of Hazardous Materials* 161: 753-9.

[21] Hameed, B. H., Krishni, R. R., and Sata, S. A. 2009. "A Novel Agricultural Waste Adsorbent for the Removal of Cationic Dye from Aqueous Solutions." *Journal of Hazardous Materials* 162: 305-11.

[22] Hameed, B. H., Mahmoud, D. K., and Ahmad, A. L. 2008. "Sorption Equilibrium and Kinetics of Basic Dye from Aqueous Solution Using Banana Stalk Waste." *Journal of Hazardous Materials* 158: 499-506.

[23] Langmuir, I. 1918. "The Adsorption of Gases on Plane Surfaces of Glass, Mica and Platinum." *Journal of the American Chemical Society* 40: 1361-403.

[24] Freundlich, H. 1906. "On Adsorption in Solution." *Z. Physik Chemical* 57: 385-471.